



Research article

Tendon stem cells seeded on dynamic chondroitin sulfate and chitosan hydrogel scaffold with BMP2 enhance tendon-to-bone healing

Qingsong Zhang^{a,b,1}, Huawei Wen^{b,1}, Guangyang Liao^b, Xianhua Cai^{a,*}^a The First School Clinical Medicine, Southern Medical University, Guangdong 510515, China^b Wuhan Fourth Hospital, Wuhan 430030, China

ARTICLE INFO

Keywords:

Tendon stem cells
Chondroitin sulfate
Chitosan
BMP2
Tendon-to-bone healing

ABSTRACT

Failure to adequately reconstruct the tendon-to-bone interface constitutes the primary etiology underlying rotator cuff retear after surgery. The purpose of this study is to construct a dynamic chondroitin sulfate and chitosan hydrogel scaffold (CHS) with bone morphogenetic protein 2 (BMP2), then seed tendon stem cells (TSCs) on BMP2-CHS for the rotator cuff reconstruction of tendon-to-bone interface. In this dynamic hydrogel system, the scaffold could not only have good biocompatibility and degradability but also significantly promote the proliferation and differentiation of TSCs. The ability of BMP2-CHS combined with TSCs to promote regeneration of tendon-to-bone interface was further verified in the rabbit rotator cuff tear model. The results showed that BMP2-CHS combined with TSCs could induce considerable collagen, fibrocartilage, and bone arrangement and growth at the tendon-to-bone interface and promote the biomechanical properties. Overall, TSCs seeded on CHS with BMP2 can enhance tendon-to-bone healing and provide a new possibility for improving the poor prognosis of rotator cuff surgery.

1. Introduction

Rotator cuff tears are commonly seen clinically. The main treatment is arthroscopic surgery, and more than 300,000 rotator cuff repair procedures are performed annually in the United States [1]. The rotator cuff insertion is composed of bone, cartilage, and tendon arranged in an orderly gradient to prevent stress concentration and complete mechanical load transmission. Unfortunately, because the healing process is located in the articular joint and affected by synovial fluid and its internal biochemical environment, it often results in poorly organized neofibrovascular scar tissue, leading to high retear rates from 30 % to 70 % [2]. In order to solve this problem, biological tissue engineering for promoting rotator cuff tendon-to-bone healing has been extensively studied. The technology requires appropriate cell sources and growth factors as well as scaffold materials with special properties. The scaffold should act as an extracellular matrix to provide the cells with mechanical support and physiochemical microenvironments.

In regard to growth factors, bone morphogenetic protein 2 (BMP2)-induced signal transduction is an important positive regulator that acts in recruitment, proliferation and differentiation of stem cells [3]. However, BMP2 injection alone cannot stably influence

* Corresponding author. The First School Clinical Medicine, Southern Medical University, No.1838 Avenue North, Guangzhou, 510515, Guangdong, China.

E-mail address: 80844942@qq.com (X. Cai).

¹ These authors contributed equally: Qingsong Zhang and Huawei Wen.

<https://doi.org/10.1016/j.heliyon.2024.e25206>

Received 23 July 2023; Received in revised form 7 December 2023; Accepted 23 January 2024

Available online 28 January 2024

2405-8440/© 2024 Published by Elsevier Ltd.

This is an open access article under the CC BY-NC-ND license

(<http://creativecommons.org/licenses/by-nc-nd/4.0/>).

tendon-to-bone healing and may result in various adverse effects, particularly extensive heterotopic ossification [4]. Therefore, in order to maintain the effective and stable functions of BMP2, some tissue engineering studies have focused on the release of growth factors from the scaffolds. Shen et al. [5] reported targeted delivery of BMP2 to stimulate osteogenesis by tethering BMP2 onto a poly scaffold using PEG as a spacer, which demonstrated the potential for biomimetic surface engineering. However, they did not have much biological information contained in the natural scaffold that cannot interact with cells ideally. Bianco et al. [6] tested a series of scaffolds with different properties and found that natural collagen hydrogel scaffolds showed significantly higher levels of osteogenic gene expression and adequate mineralization, which provided a reference for our scaffold design. In addition, it has been suggested that hydrogels formed through stable covalent cross-linking of polymers can limit the interaction between the cells and scaffold, which hinders the normal functions of the cells [7]. In two previous experiments, dynamic structural hydrogels were designed using reversible chemical and physical cross-linking, which achieved promising results [8,9]. Therefore, we developed a collagen-based dynamic chondroitin sulfate and chitosan hydrogel scaffold (CHS). It is critical to implant appropriate stem cells into CHS for early tendon-to-bone healing. Bone marrow mesenchymal stem cells (BMSCs) are commonly used for tendon-to-bone healing. However, it has been reported that the effects of BMSCs in improving tendon-to-bone healing were not significant at 4 weeks [10]. Recent studies have shown that tendon stem cells (TSCs) express higher levels of tenomodulin (Tnmd), collagen type I (COL-I), and scleraxis (Scx) than BMSCs, which are more favorable for formation of the tendon-to-bone interface [11]. In addition, TSCs express higher levels of BMP receptors and exhibit more osteogenic differentiation upon BMP-2 stimulation [12]. Therefore, we chose to load CHS with BMP2, seed TSCs into BMP2-CHS, and test the triad in tendon-to-bone healing. This study aims to determine the effects of TSCs seeded on BMP2-CHS on tendon-to-bone healing in a rabbit rotator cuff repair model.

2. Materials and methods

2.1. Hydrogel fabrication

As described in the previous experiments, the scaffold was prepared using Schiff's base reaction process [8,9]. First, 20 % solution A was prepared by dissolving aminated chondroitin sulfate in buffer at 75 °C. Chitosan was dissolved in buffer at 75 °C to prepare 20 % solution B. The collagen II was dissolved in buffer PH = 3.5 to prepare 20 % solution C. A solution of chondroitin sulfate containing oxidized aldehydes was dissolved in buffer at 75 °C to prepare solution D at 20 %. Second, all solutions (A to D) were mixed and BMP2 (Procell, Wuhan, China) solution was added to ensure uniform distribution. Finally, N-(3-sulfur dioxide ethyl)-3,5-sulfur dioxide phenol was added to trigger reaction, and amino- and aldehyde-chondroitin sulfate were cross-linked to form a hydrogel at 75 °C. All hydrogels were sterilized using ultraviolet light and alcohol, and washed with sterile phosphate-buffered saline (PBS) solution before use (Fig. 1). Gels were cut into pieces with a 7-mm size, hydrated through sterile PBS prior to TSCs seeding.

2.2. Scanning electron microscopy (SEM) of CHS implanted with TSCs

CHS was examined under a JEOL (Tokyo, Japan) SEM with an accelerating voltage of 3.0 kV [Fig. 2A, B]. The surface pore interconnectivity and morphology were determined by SEM and pore length was calculated using ImageJ software along with the long axis of the individual pores.

2.3. Biodegradation rate, cell viability, and releasing capacity

Rat tendon fibroblasts (L929) and human umbilical endothelial cells (HUVECs) were used to study cytocompatibility of CHS.

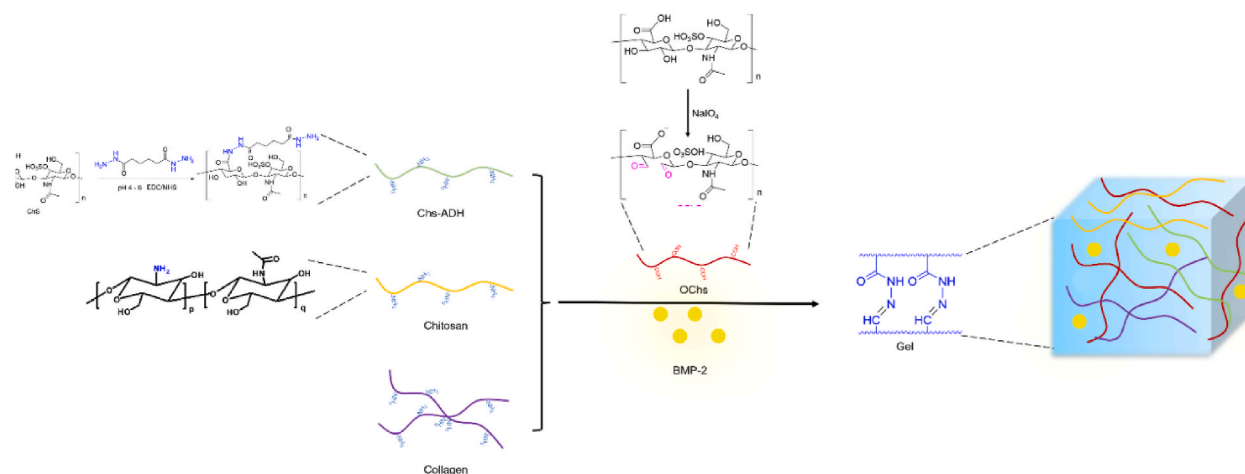


Fig. 1. Process of construction of collagen-based dynamic chondroitin sulfate and chitosan hydrogel scaffold.

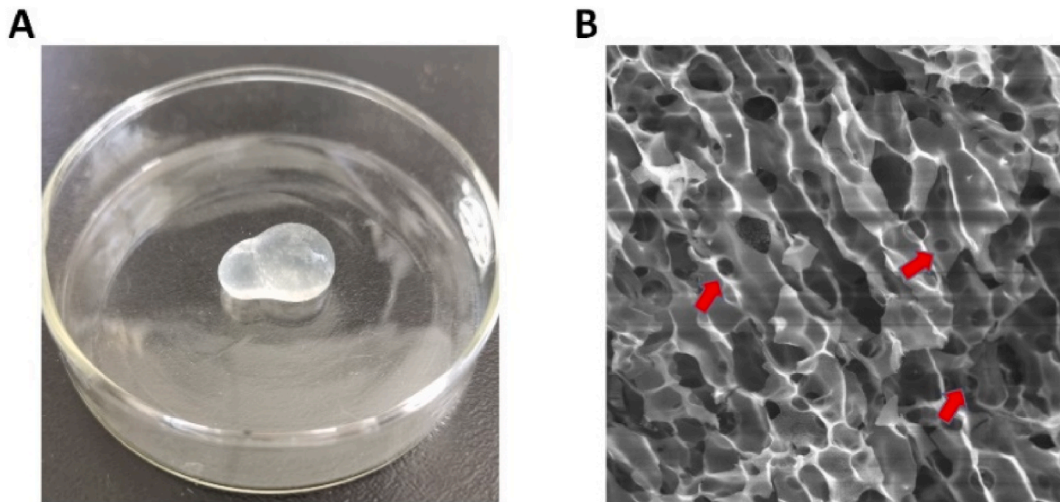


Fig. 2. Macroscopic and microscopic images of the dynamic chondroitin sulfate and chitosan hydrogel scaffold (CHS). (A) A representative macroscopic picture of CHS. (B) Scanning electron microscopy showed that CHS had a typical highly porous microstructure with a pore diameter of 50–90 μm . A few cells were observed to attach to CHS. CHS, collagen-based dynamic chondroitin sulfate and chitosan hydrogel scaffold.

Commercially available L929 and HUVECs were purchased from Procell (Wuhan, China). Cells were cultured in CHS supplemented with 10 % FBS, 1 % antibiotics and antimycotic solution in the incubator at 37 °C under a humidified 5.0 % CO_2 atmosphere. To further investigate the biocompatibility of CHS, gels were placed in 24-well culture plates, and cells were seeded onto the gels and cultured for indicated periods. BMP2-CHS was cultured in Dulbecco's modified Eagle medium at 37 °C under a humidified 5.0 % CO_2 atmosphere, and BMP2 release capacity was measured by BMP2 ELISA assay kit.

2.4. TSCs isolation and culture

The tendons used for cell extraction were removed from the rotator cuff of 6 male adult rabbits. The tendons were chopped and digested with type I collagenase (3 mg/mL), and the released cells were washed with PBS and suspended in Dulbecco's modified Eagle medium. The isolated nucleated cells were plated at a low density (500 cells/ cm^2) and cultured at 37 °C and 5 % CO_2 to form colonies. After 3 days of initial culture, the non-adherent cells were removed. From the 7th to 10th day, the cell colonies were trypsin-digested and mixed, which were named as the zero generation (P_0) of TSCs. The TSCs were subcultured at a density of 4000 cells/ cm^2 . The stem cell characteristics of TSCs were routinely confirmed by its clonality and multi-directional differentiation potential [13,14].

2.5. TSCs seeding to CHS

CHS was placed into each well of a non-treated 24-well polystyrene plate and the growth medium was added for 2 h. The cell suspension (10 μl with 2×10^4 TSCs) was seeded onto CHS for 1 h. Then, 1 mL of growth medium was added to each well. The TSCs-seeded scaffolds were placed at 37 °C in a humidified incubator with 5 % CO_2 for one day to allow the cells to adhere. Seven days later, the growth medium was changed to saline before transplantation in the animal experiments.

2.6. Adhesion and proliferation of TSCs in CHS

The morphology of TSCs grown on CHS was examined directly using an inverted microscope. Population doubling time (PDT) was determined to assess the proliferative capacity of these cells on CHS according to the method previously published [14]. For H&E staining, TSCs grown in CHS were fixed with 4 % paraformaldehyde for 30 min at room temperature. Subsequently, the CHS with TSCs was placed in pre-labeled base molds filled with frozen section medium. The base mold with CHS and TSCs was quickly immersed in liquid nitrogen cooled 2-methylbutane and allowed to solidify completely. The CHS-TSCs block was cut into 10 μm thick sections, and the sections were rinsed three times with PBS and stained with H&E.

2.7. In vitro expression of differentiation markers of TSCs

Gene expression of differentiated TSCs grown on the surface of CHS was determined by qRT-PCR. Total RNA was extracted with a RNeasy Mini Kit with an on-column DNase I digest (Qiagen). The qRT-PCR was carried out using QIAGEN QuantiTect SYBR Green PCR Kit (Qiagen). In a 50 μl PCR reaction mixture, 2 μl cDNA (total 100 ng RNA) was used to check expression of the markers of TSCs. Alkaline phosphatase (ALP), dwarf-associated transcription factor 2 (Runx2), and osteocalcin (OCN) are markers of osteogenic differentiation. Tenocyte-related genes include collagen type I, collagen type III, and tenomodulin. Expression of related genes in

fibrocartilage includes CD80, glycosaminoglycan (GAG) core protein, and collagen type II. Rabbit specific primers were used to detect gene expression of these markers at different times. Glyceraldehyde-3-phosphate dehydrogenase (GAPDH) was used as internal reference. All the primers were synthesized by Invitrogen (Qiagen).

2.8. In vivo study design

All methods are reported in accordance with ARRIVE guidelines. Adult male New Zealand rabbits ($n = 37$, six-months old, with a body weight of 3–3.5 kg) were used and the rabbits were divided into four groups (totally $n = 9$ per group): 1) suture only, 2) suture plus CHS, 3) suture plus BMP2-CHS, and 4) suture plus BMP2-CHS with TSCs. Rabbits from each group were euthanized at 6 or 12 weeks for histologic evaluation ($n = 3$ per time point per group) and 12 weeks for biomechanical evaluation ($n = 3$ per group) postoperatively. One animal was put in the suture plus CHS group and harvested at day 1 to check whether the implant was located in the right place between the supraspinatus tendon and the bone postoperatively.

2.9. Surgical procedures

All rabbits underwent bilateral surgeries to transect and repair the supraspinatus tendon at its insertion site. Briefly, after inhaling 1%–5% isoflurane to induce anesthesia followed by general anesthesia with an intraperitoneal injection of pentobarbital (12–15 mg/kg), a 1.5-cm longitudinal anterolateral skin incision was made on the shoulder; the deltoid muscle was split; and the supraspinatus tendon and greater tuberosity were exposed. The supraspinatus tendon was sharply detached at the insertion site and any remaining fibrocartilage on the great tuberosity was removed with a scalpel. A 1.0-mm in diameter bone tunnel was created at the center of the footprint through the lateral cortical bone. The transected supraspinatus tendon was repaired back to its insertion on the greater tuberosity with a #1–0 polypropylene suture by passing the suture ends from the tendon through the bone tunnel. The skin incision was closed with #2–0 nylon sutures. After the rabbits woke up after surgery, meloxicam (0.2 mg/kg) was injected subcutaneously for 3 days for analgesia. All rabbits were permitted cage activities without immobilization [Fig. 3A, B].

2.10. Histological evaluation

Euthanasia was performed at 6 and 12 weeks postoperatively through overdose of pentobarbital sodium (50 mg/kg). The bilateral shoulders of 9 rabbits from each group were evaluated. After fixation and decalcification, specimens were bisected along the long axis of the tendon to expose the tendon-to-bone connection, and then paraffin-embedded to prepare 4- μ m-thick sections. The tissue sections were stained with H&E to examine the morphologic characteristics, stained with Masson trichrome to examine the fibrocartilage

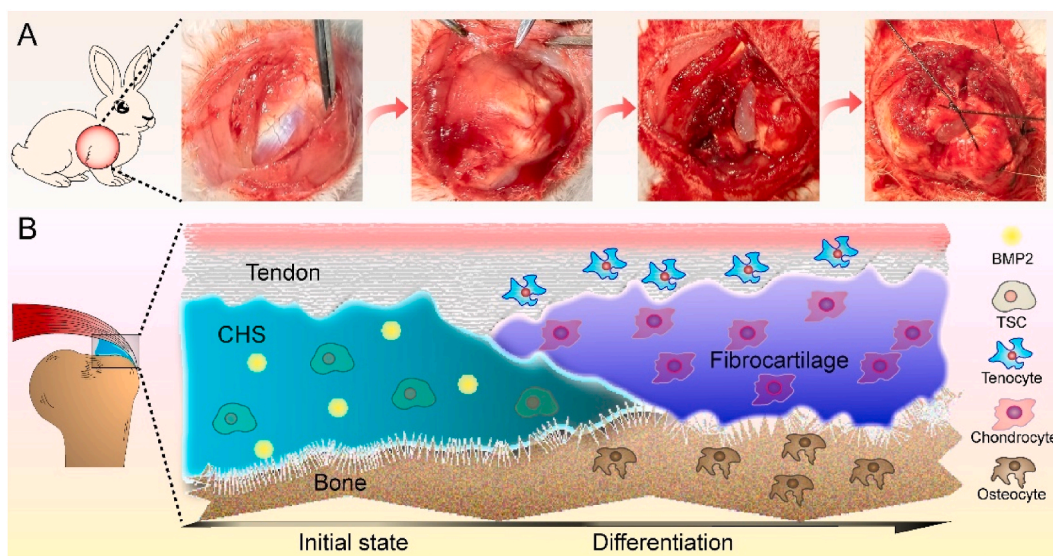


Fig. 3. BMP2-CHS with TSCs for regeneration of tendon-to-bone interface in acute rotator cuff tear model. (A) Illustration of a surgical procedure showing the CHS incorporated into the bony rough on the greater tuberosity and suturing of the transected supraspinatus tendon to its anatomic position, using #1–0 polypropylene horizontal mattress sutures passing through the bone tunnels. From left to right: rabbit shoulder was shaved and prepared; the deltoid muscle was split to expose the supraspinatus tendon; the rotator cuff was completely exposed; the supraspinatus tendon at attachment site of the great tuberosity was transected and the stent was implanted; the transected supraspinatus tendon and the stent were sutured together and re-attached onto the greater tuberosity. (B) A hypothetical model of how BMP2-CHS promotes differentiation of TSCs into tenocytes, chondrocytes and osteocytes, to improve tendon-to-bone healing. CHS, collagen-based dynamic chondroitin sulfate and chitosan hydrogel scaffold; BMP2, bone morphogenetic protein 2; TSCs, tendon stem cells.

distribution, and stained with Picrosirius red to examine the collagen fiber organization. The sections were viewed under a Nikon Eclipse E100 microscope (Nikon Corporation, Tokyo, Japan), and digital images were taken using a Nikon DS-U3 camera on the microscope (Nikon Corporation). Computerized image analysis was performed using Image J (National Institutes of Health, Bethesda, MD) to evaluate the repair outcomes including cellularity, vascularity, and collagen fiber orientation in a semi-quantitative manner. A modified histologic scoring system was used for each parameter (Table 1).

2.11. Biomechanical evaluation

Six shoulders from each group were tested for biomechanical properties 12 weeks after the surgery. All fresh specimens were frozen at -80°C until testing. After thawing, the grafted tendon to the humerus was dissected from the surrounding tissues and the supraspinatus muscle belly and any scar tissue were removed. Each specimen was preloaded to 10 N and then loaded to failure with a conventional tensile tester (STA1225; Orientec, Tokyo Japan) at a rate of 5 mm/s, and the ultimate load to failure and the failure site were recorded.

2.12. Statistical analysis

All statistical data were analyzed using SPSS software version 26.0 (IBM, Chicago, USA). All experiments were implemented at least three times, and the data were presented as the mean \pm standard deviation. If the data were normally distributed, Student's *t* tests (two-tailed) and one-way analysis of variance (ANOVA) were performed to assess the statistical difference. $P < 0.05$ was considered statistically significant. Power analysis was used to assess sample size, and power values > 0.80 was considered that the sample size was for each group.

3. Results

3.1. Biodegradation rate, cell viability, and releasing capacity in vitro

We found that within 30 days, the scaffold was degraded at a rate of about 2.5 % per day, and there was almost no residue after 60 days (Fig. 4A). When the cells were cultured with the scaffold for 24 and 48 h, the survival rates of HUVEC and L929 cells were approximately 100 %, indicating that the scaffolds showed great cytocompatibility (Fig. 4B). The scaffold released BMP2 at a rate of 1 % per hour for 2 days, then at a rate of 7.3 % per day until it leveled off on the fifth day, with a cumulative release rate of 70 % (Fig. 4C).

3.2. Adhesion and proliferation of TSCs in CHS

After 24 h in culture, the results of inverted microscopy showed that the TSCs grew on CHS surface (Fig. 4D). Frozen sections with H&E staining showed that TSCs migrated into the inside of CHS (Fig. 4E). In addition, TSCs grew faster in CHS than on plastic surfaces, as shown by the population doubling times (PDTs) of TSCs on these two substrates (Fig. 4F). The PDT of TSCs in CHS was about 16.5 % lower than that on the plastic surfaces. As a result, TSCs formed larger colonies on CHS compared to TSCs grown on the plastic surfaces within the same culture time.

3.3. Tenogenic, chondrogenic and osteogenic differentiation of TSCs

We examined the multi-differentiation potential of TSCs using qRT-PCR by culturing them in tenogenic, chondrogenic, and osteogenic induction media, respectively. Three sets of genes included tenocyte-related genes (collagen I, collagen III, and tenomodulin), chondrocyte-related genes (CD80, GAG core protein, and collagen II), and osteocyte-related genes (ALP, Runx2, and OCN) [Fig. 5(A-D)]. We found that all chondrocyte-related and osteocyte-related genes were significantly up-regulated in TSCs cultured in CHS and BMP2-CHS compared to those on the plastic surface. Expression of tenocyte-related genes (collagen III and tenomodulin, except collagen I) was not significantly different between CHS and BMP2-CHS. Expression of chondrocyte-related genes (GAG and

Table 1
Semi-quantitative histologic scoring system.

Parameter	Scores			
	1	2	3	4
Cellularity, % ^a	>400	300–400	200–300	<200
Vascularity, bv/low PF	>15	11–15	6–10	<6
Collagen fiber orientation, % ^b	<25	25–50	50–75	>75

bv, blood vessel; PF, power field (low PF = 100-fold magnification).

^a Number of cells per region of interest from each section. The percentages represent relative values compared with the values from the normal tendon-to-bone sections ($n = 3$), which were set at 100 %.

^b Grayscale per region of interest from each section as measured using Image J. The percentages represent relative values compared with the values from the normal tendon-to-bone sections ($n = 3$), which were set at 100 %.

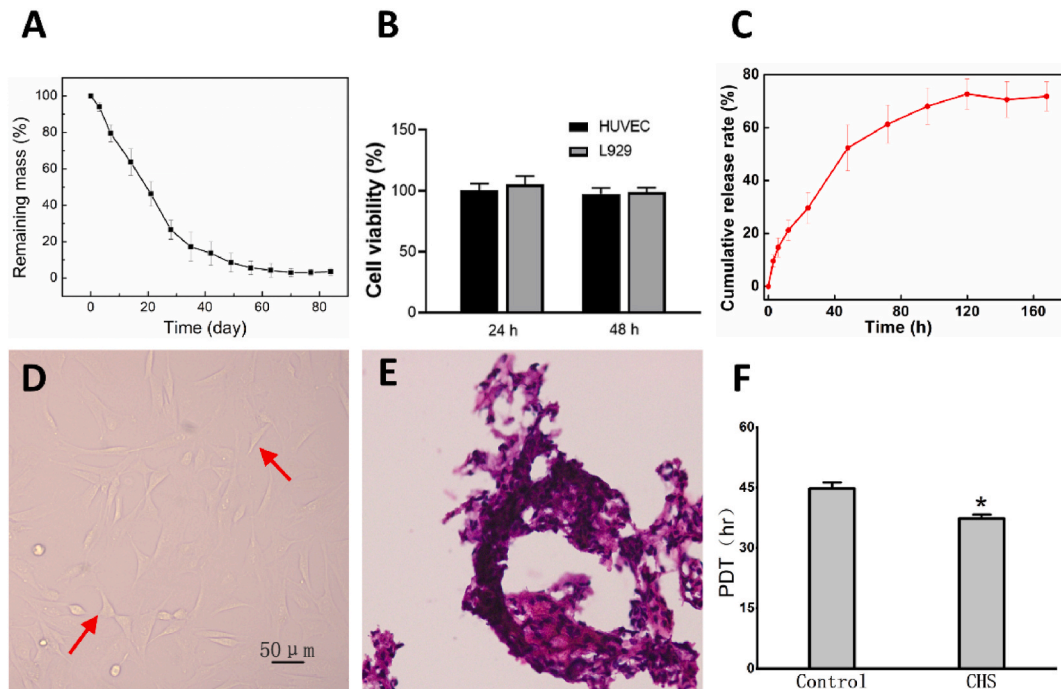


Fig. 4. (A) The relationship between degradation time and remaining mass of CHS. (B) The relationship between cell incubation time and cell viability. (C) The binding and releasing capacity of BMP2-CHS. (D) TSCs examined under an inverted microscope. (E) Frozen sections showed that TSCs had migrated into the inside of CHS. (F) The population doubling time (PDT) of TSCs on CHS was significantly lower than that of the same cells on the culture plate surface (* $p < 0.05$). CHS, collagen-based dynamic chondroitin sulfate and chitosan hydrogel scaffold; TSCs, tendon stem cells. HUVEC, human umbilical vein endothelial cell; L929, mouse fibroblasts cell.

collagen II, except CD80) was highly increased in BMP2-CHS compared to those in CHS. Expression of osteocyte-related genes (ALP, Runx2, and OCN) in CHS and BMP2-CHS was notably higher than those in CHS. These results manifested that CHS could improve differentiation of TSCs into tenocytes, chondrocytes, and osteocytes. Moreover, BMP2 might promote TSCs differentiation to chondrocytes under certain circumstances and could markedly promote TSCs differentiation into osteocytes.

3.4. H&E staining

At 6 weeks, we observed highly vascularized and disorganized granulation tissues in the control group. Dense and disordered collagen fibers were formed in both the CHS group and the BMP2-CHS group, and the histologic findings were similar among the two groups. The orientation of collagen fibers tended to be organized at the insertion site with a certain degree of order in the BMP2-CHS with TSCs group (Fig. 6). At 12 weeks, the specimens showed that the formation of collagen fibers was denser, and the collagen improvement at the insertion site was particularly obvious and more orderly. Furthermore, we found a relatively clear three-layer structure at the interface of the tendon-to-bone.

3.5. Masson trichrome staining

At 6 weeks, there was no fibrocartilage formation at the tendon-to-bone interface in the control group. A little fibrocartilage formation was found in the other three experiment groups, which was firmly continuous with the tendon and bone tissue, but there was no significant difference in the amount of new fibrocartilage among the 3 groups (Fig. 7).

At 12 weeks, there was still no fibrocartilage formation in the control group. The amount of fibrocartilage in the CHS group did not increase significantly compared to 6 weeks. The amount of fibrocartilage in the BMP2-CHS group and the BMP2-CHS with TSCs group was increased significantly compared to 6 weeks, but there was no significant difference between the BMP2-CHS group and the BMP2-CHS with TSCs group.

3.6. Picrosirius red staining illuminated with polarized light

We found that the orientation of collagen fibers in the tendon-to-bone insertion site of any of groups tended to be more organized at 12 weeks compared to 6 weeks. At 6 and 12 weeks, the areas of brightly diffracted polarized light were rarely seen at the tendon-to-bone interface in the control group, and a small area of unordered brightly diffracted polarized light could be seen in the CHS group.

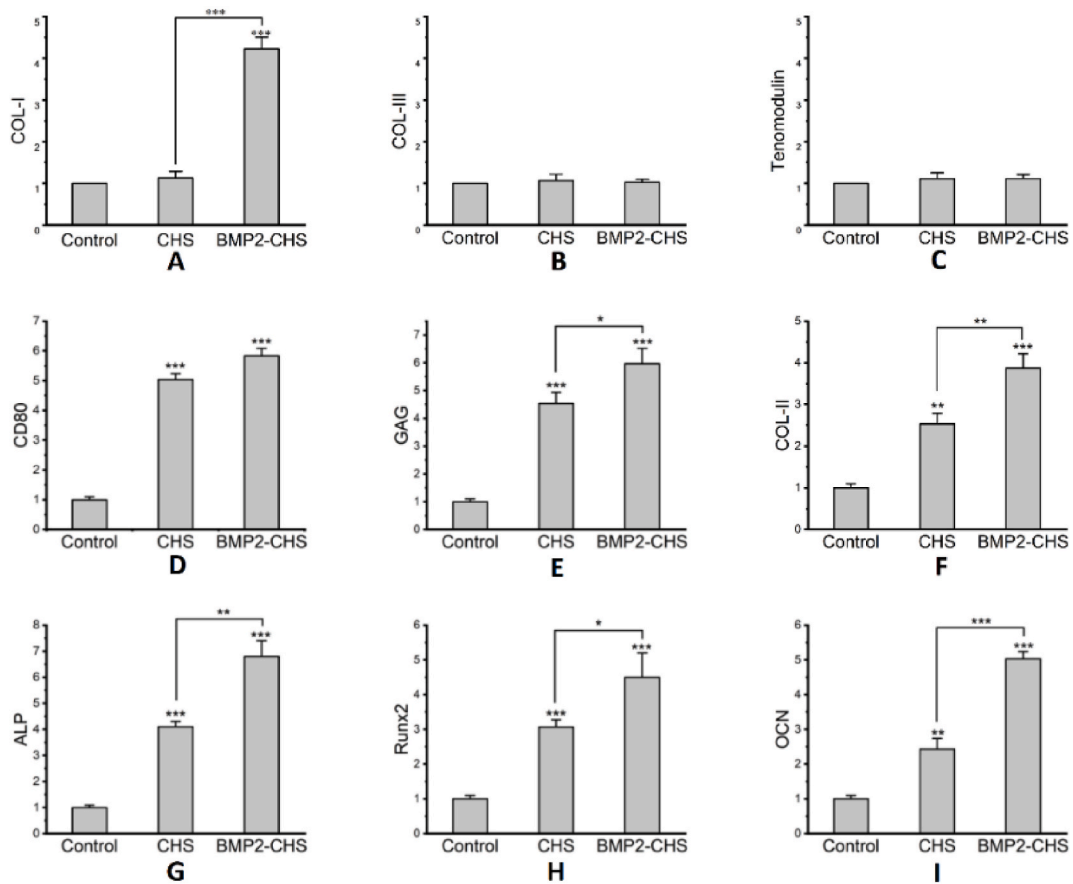


Fig. 5. Multi-differentiation potential of TSCs in CHS, BMP2-CHS, and on control plastic surface. After being cultured in respective induction media for 7 days, expression of tenocyte-related, chondrocyte-related, and osteocyte-related genes in CHS and BMP2-CHS was significantly higher than those on control plastic surface. (A to C) Expression of COL-I, COL-III, and Tenomodulin. (D to F) Expression of CD80, GAG core protein, and COL-II. (G to I) Expression of ALP, Runx2, and OCN. * $p < 0.05$, ** $p < 0.1$, and *** $p < 0.001$ compared with each control group unless marked by a horizontal line. Note that the gene expression levels were normalized with respect to their controls. CHS, collagen-based dynamic chondroitin sulfate and chitosan hydrogel scaffold; BMP2, bone morphogenetic protein 2; TSCs, tendon stem cells.

The area of brightly diffracted polarized light at the tendon-to-bone interface in the BMP2-CHS group and BMP2-CHS with TSCs group was significantly larger than that in the other groups, but there was no significant difference between the BMP2-CHS group and BMP2-CHS with TSCs group (Fig. 8).

3.7. Histologic evaluation

Six shoulders from each group were evaluated at 6 and 12 weeks postoperatively. The results of semiquantitative histologic evaluation are presented in Table 2.

Cellularity. The cellularity decreased significantly over time in Group 1 (6 vs 12 weeks, $P < 0.001$), Group 2 (6 vs 12 weeks, $P < 0.001$), Group 3 (6 vs 12 weeks, $P < 0.001$), and Group 4 (6 vs 12 weeks, $P = 0.001$). At 6 weeks, the cellularity was significantly lower in Group 4 ($P = 0.048$ vs. Group 1, $P = 0.002$ vs. Group 2, and $P < 0.001$ vs. Group 3). However, there was no significant difference among the groups at 12 weeks (Group 4 vs Group 1, $P = 0.771$; Group 4 vs Group 2, $P = 0.429$; and Group 4 vs Group 3, $P = 0.343$).

Vascularity. The number of blood vessels was significantly different with respect to the time points in Group 1 (6 vs 12 weeks, $P = 0.002$), Group 2 (6 vs 12 weeks, $P = 0.003$), Group 3 (6 vs 12 weeks, $P = 0.004$), and Group 4 (6 vs 12 weeks, $P = 0.009$). In Group 4, it decreased significantly compared with Group 1 ($P = 0.006$), although not with Group 2 ($P = 0.248$) or Group 3 ($P = 0.342$) at 6 weeks. Similarly, the number of blood vessels of Group 4 decreased significantly compared to Group 1 ($P = 0.019$), although not with Group 2 ($P = 0.478$) or Group 3 ($P = 0.730$) at 12 weeks.

Collagen Fiber Orientation. Measured on the grayscale, the value of collagen fiber orientation significantly increased over time in Group 1 (6 vs 12 weeks, $P = 0.001$), Group 2 (6 vs 12 weeks, $P = 0.001$), Group 3 (6 vs 12 weeks, $P = 0.001$), and Group 4 (6 vs 12 weeks, $P = 0.002$). There were significant differences among the groups at 6 weeks (Group 4 vs Group 1, $P < 0.001$; Group 4 vs Group 2, $P < 0.001$; and Group 4 vs Group 3, $P = 0.002$). And, there were significant differences among the groups at 12 weeks (Group 4 vs

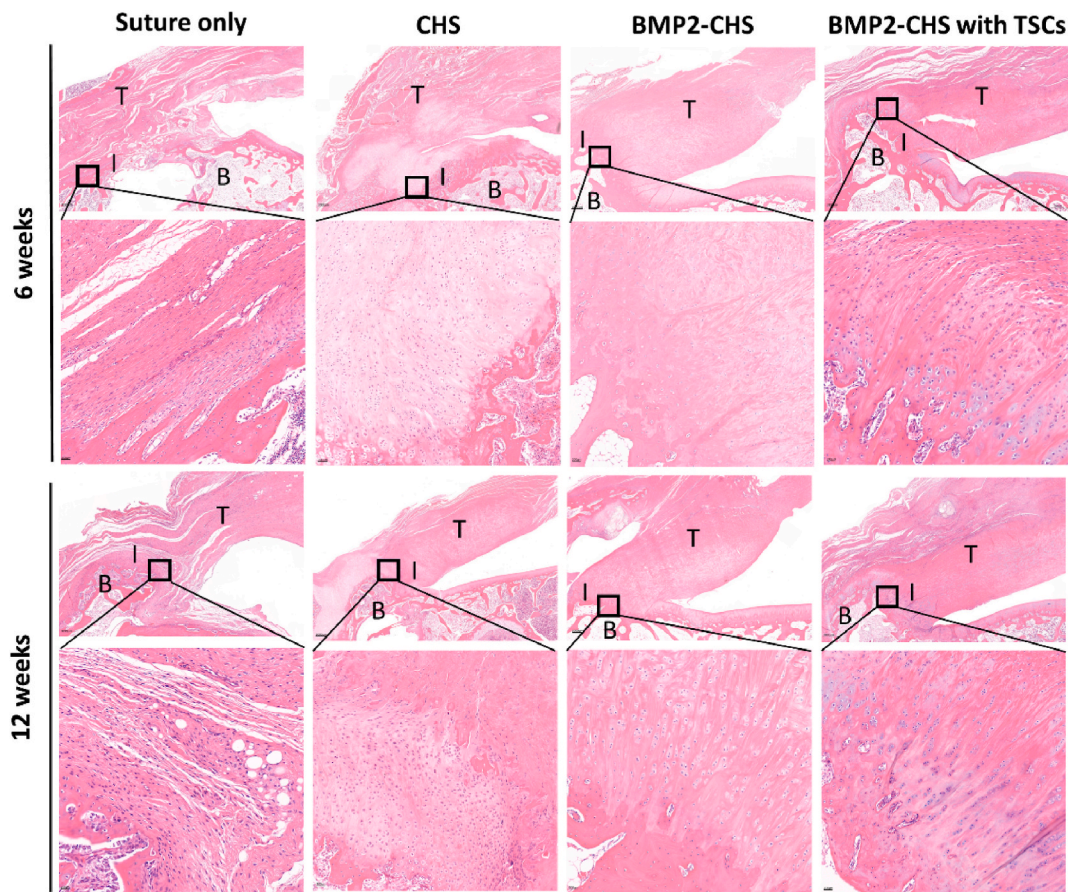


Fig. 6. Photomicrographs of the tendon-to-bone interface in the 4 groups, taken at 6 and 12 weeks after surgery after H&E staining. The boxed areas in the upper images from each group at each time point are shown at a higher magnification in the lower panel. CHS, collagen-based dynamic chondroitin sulfate and chitosan hydrogel scaffold; BMP2, bone morphogenetic protein 2; TSCs, tendon stem cells; T, tendon; B, bone; I, interface.

Group 1, $P = 0.002$; Group 4 vs Group 2, $P = 0.018$), except for Group 4 vs group 3 ($P = 0.061$).

Total histologic score. The total histologic score was significantly increased over time in Group 1 (6 vs 12 weeks, $P < 0.001$), Group 2 (6 vs 12 weeks, $P < 0.001$), Group 3 (6 vs 12 weeks, $P < 0.001$), and Group 4 (6 vs 12 weeks, $P = 0.001$). At 6 weeks, the total score was significantly higher in Group 4 than Group 1 ($P < 0.001$), Group 2 ($P = 0.001$), and Group 3 ($P = 0.001$). And similarly, it was significantly higher among the groups at 12 weeks (Group 4 vs Group 1, $P < 0.001$; Group 4 vs Group 2, $P = 0.022$; and Group 4 vs Group 3, $P = 0.046$).

3.8. Biomechanical testing

We tested 24 specimens (6 shoulders from each group) from the supraspinatus tendon-to-bone repair constructs at 12 weeks postoperatively. All experimental specimens failed at the repair site during testing. At 12 weeks, the ultimate load to failure was 71.44 ± 13.54 N in Group 1, 91.76 ± 5.15 N in Group 2, 116.78 ± 15.5 N in Group 3, and 129.34 ± 7.62 N in Group 4. The ultimate load to failure was significantly higher in Group 4 than Group 1 ($p < 0.001$) and Group 2 ($p < 0.001$); however, no significant difference in the ultimate load to failure of the repair site was observed between Group 3 and Group 4 ($p = 0.105$).

4. Discussion

In this study, we developed a biodegradable hydrogel scaffold, or CHS, by polymerizing chondroitin sulfate and chitosan according to an aldehyde-polycondensation reaction, using collagen as a matrix to form a scaffold with specific physical and biological properties. Collagen provides structural stability and elasticity, while chondroitin sulfate and chitosan are responsible for retaining moisture and providing dynamic stability. The principal finding of this study was that CHS could be combined with a growth factor to induce stem cell proliferation and differentiation, improve the biological process of tendon-to-bone healing, and increase the biomechanical strength of tendon-to-bone connections.

Many studies have demonstrated that BMP2 plays an important role in the transduction pathway as a positive regulator of

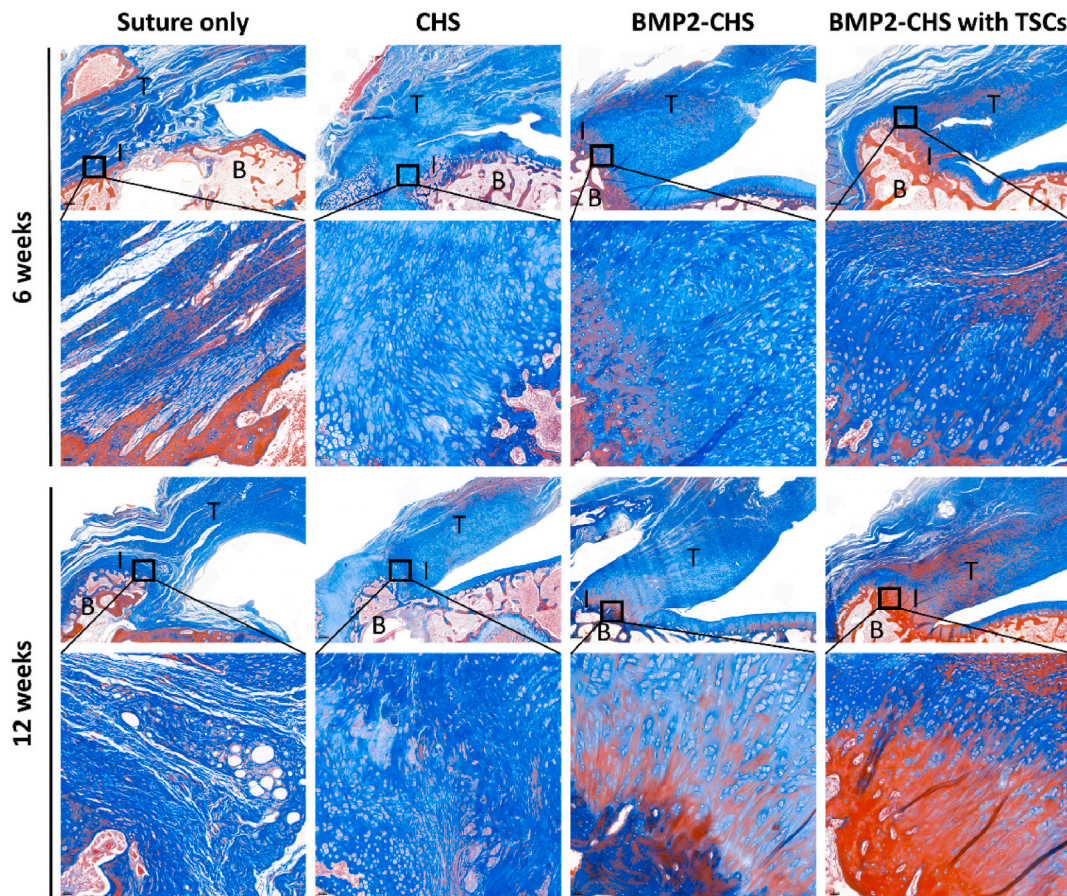


Fig. 7. Photomicrographs of the tendon-to-bone interface in the 4 groups, taken at 6 and 12 weeks after surgery after Masson trichrome staining. The boxed areas in the upper images from each group at each time point are shown at a higher magnification in the lower panels. CHS, collagen-based dynamic chondroitin sulfate and chitosan hydrogel scaffold; BMP2, bone morphogenetic protein 2; TSCs, tendon stem cells; T, tendon; B, bone; I, interface; F, fibrocartilage.

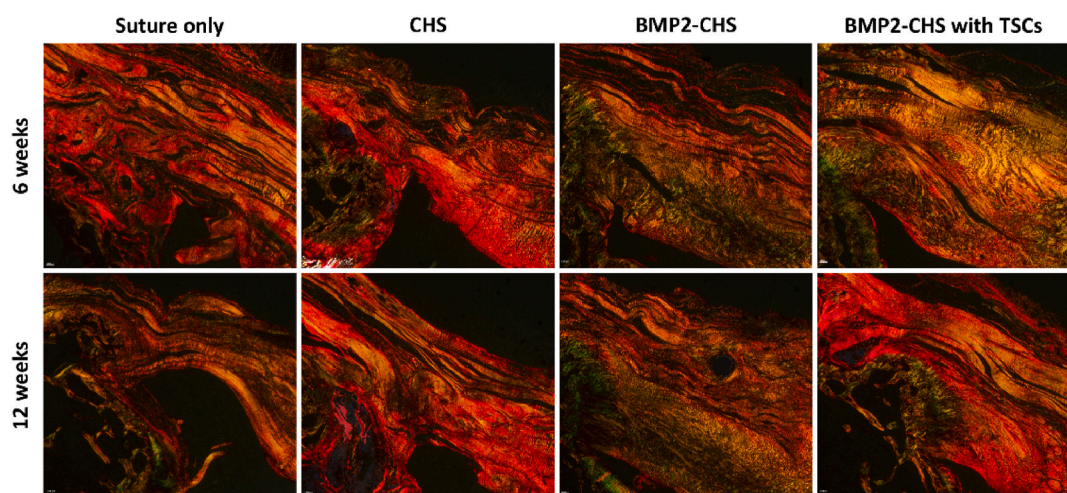


Fig. 8. Photomicrographs of the tendon-to-bone interface in the 4 groups, taken at 6 and 12 weeks after surgery after picrosirius red staining with illumination of polarized light. CHS, collagen-based dynamic chondroitin sulfate and chitosan hydrogel scaffold; BMP2, bone morphogenetic protein 2; TSCs, tendon stem cells; T, tendon; B, bone; I, interface.

Table 2
Results of histologic evaluation.

Groups	Cellularity, % ^a	Vascularity, bv/low PF ^c	Collagen fiber orientation, % ^d	Total score ^e
At 6 weeks				
Group 1	342 ± 43.9	18.5 ± 5.1	49.3 ± 5.8	5.8 ± 0.8
Group 2	403 ± 49.1	12.5 ± 4.7	55.3 ± 4.1	6.3 ± 1.0
Group 3	461 ± 49.8	11.8 ± 4.4	58.3 ± 7.3	6.5 ± 1.0
Group 4	279 ± 52.2 ^{#- -ξ}	9.5 ± 3.7 [#]	76.8 ± 7.8 ^{#- -ξ}	8.8 ± 0.8 ^{#- -ξ}
At 12 weeks				
Group 1	208 ± 36.6	12.2 ± 3.4	63.8 ± 9.6	8.7 ± 0.8
Group 2	222 ± 48.4	8.5 ± 3.4	71.3 ± 8.6	9.7 ± 1.0
Group 3	228 ± 54.4	7.8 ± 3.7	72.8 ± 11.7	9.7 ± 1.2
Group 4	202 ± 32.9	7.2 ± 2.8 [#]	85.2 ± 8.3 ^{#-}	11 ± 0.6 ^{#- -ξ}

NOTE. n = 6 for all groups. Values are expressed as the mean ± standard deviation. Group 1 = suture only; Group 2 = suture plus CHS; Group 3 = suture plus BMP2-CHS; and Group 4 = suture plus BMP2-CHS with TSCs.

bv, blood vessel; BMP2, bone morphogenetic protein 2; CHS, collagen-based dynamic chondroitin sulfate and chitosan hydrogel scaffold; TSCs, tendon stem cells.

^{#-||-ξ} Significantly different between groups compared with Group 1 ([#]), Group 2 (^{||}), and Group 3 (^ξ) at the same time point ($P < 0.05$).

^a Number of cells per region of interest from each section. The percentages represent relative values compared with the values from the normal tendon-to-bone sections (1268 ± 148 cells/mm² n3), which were set to 100 %.

^c Number of blood vessels per low power field (100x magnification) from each section.

^d Grayscale per region of interest from each section as measured using Image J. The percentages represent relative values compared with the values from the normal tendon-to-bone sections (144.67 ± 17.78 grayscale, n = 3), which were set to 100 %.

^e Scores represent a total score of three parameters, including cellularity, vascularity, and collagen fiber orientation.

osteoblast differentiation, which can induce bone formation and enhance tendon-to-bone healing [4,15]. Because growth factors cannot effectively act at the tendon-to-bone interface alone, they are often loaded on various biomaterials. At present, the research of biomaterials is mainly based on synthetic scaffolds such as poly-glycolic-acid and poly-L-lactic-acid [16,17], and natural scaffolds such as silk and collagen [18,19], both of them having their own advantages and disadvantages. Compared with synthetic scaffolds, natural scaffolds contain a lot of biological information, and some specific amino acid sequences can interact with cells [20,21]. Moreover, natural scaffolds can be hydrolyzed or degraded by enzymes, thereby avoiding the toxicity of the scaffolds and chronic immune responses from the body [22]. Therefore, we thought that natural scaffold could perform greater functions at the rotator cuff insertion. Hydrogels have attracted extensive attention in the field of tendon-to-bone healing due to their ability to simulate the microscopic dynamic structural characteristics of extracellular matrix [23]. Previous studies have shown that chondroitin sulfate could induce new bone formation and promote cartilage regeneration in vivo [24]. Besides, chondroitin sulfate could inhibit the activity of natural killer cells and elastase and improve the healing process [25]. Chitosan from natural sources contains intrinsic amine groups, and the aldehyde groups obtained by amidation can directly participate in the Schiff's base reaction, making it an ideal material for the preparation of dynamic hydrogels [26]. Collagen is the main component of the tendon-to-bone interface, providing essential structural stability [27,28]. Based on these considerations, we prepared a collagen-based dynamic chondroitin sulfate and chitosan hydrogel scaffold.

We speculated that after application of CHS or BMP2-CHS, the tendon-to-bone interface would be more quickly filled with tendon, cartilage and bone tissue, and the biomechanical strength would be significantly enhanced. Our histological results showed that after application of CHS and BMP2-CHS, the number of vertical collagen fibers in the insertion increased and fibrocartilage attachment and bone regeneration were promoted. The healing tissue gradually grew, mineralized, and fused together, forming a continuous but clear structure over the time. More importantly, more new bone tissue formation was founded in BMP2-CHS group than CHS group. This might be related to the mechanism of BMP2 inducing the differentiation and proliferation of stem cells into chondroblasts and osteoblasts [29]. ALP is an early marker of osteoblast differentiation and maturation [30]. Runx2 is expressed in the early stage of healing and plays an important role in osteoblast differentiation and development [31]. OCN is expressed during osteogenic differentiation and mineralization [32]. In this study, the gene expression levels of ALP, Runx2 and OCN in BMP2-CHS group were higher than those in CHS group. This result was consistent with the findings of Arvinus et al. [33] that BMP2 significantly increased the expression of osteoblast marker genes. Furthermore, we found that the expression of bone formation markers in CHS group was significantly higher than that in control group, which may be related to the effect of chondroitin sulfate to promote osteocyte proliferation and the reticular structure of collagen to accelerate osteoblast mineralization. Generally speaking, the presence of fibrocartilage tissue can enhance the adhesion of the tendon-to-bone interface by increasing the pullout strength [34]. As a component of cartilage tissue, chondroitin sulfate can also promote the formation of cartilage matrix [24,25]. CD80 and COL-II are expressed during chondrocyte regeneration [35,36]. Chondroitin sulfate is a kind of GAG [37]. In this study, we found that the gene expression of CD80, GAG core protein, and COL-II increased significantly. In addition, a small amount of fibrocartilage was found in both CHS group and BMP2-CHS group at 6 weeks after surgery and was closely connected with tendon and bone tissue. At 12 weeks after surgery, there was no significant increase in the amount of fibrocartilage in CHS group, but the amount of fibrocartilage increased significantly in BMP2-CHS group. It may be related to the synergistic induction of chondrogenic differentiation and proliferation of stem cells by BMP2 and chondrocytes. These results suggest that both CHS and BMP2-CHS could induce the formation of chondrocytes and promote tendon-to-bone healing. Arvinus et al. [33] proposed that BMP2 enhanced tendon-to-bone healing by increasing the activity of tendon cells and the expression

and production of type I collagen. In this study, the gene expression level of type I collagen in BMP2-CHS group was significantly higher than that in control group and CHS group, which may be the result of up-regulation of type I collagen expression promoted by BMP2. Type III collagen is also the main collagen in the tendon [38]. Tenomodulin is highly expressed in tendon tissues and is an important factor in tendon cell maturation [39]. However, there was no significant difference in the expression of COL-III and Tenomodulin among the three groups. This might indicate that BMP2 and CHS have limited effect on TSCs. Nevertheless, the histological results showed that the number of vertical collagen fibers was increased in the insertion, which might be related to the characteristics of TSCs. This was consistent with the high expression levels of tenogenic genes in three groups. TSCs isolated from the tendons are mesenchymal stem cells with multi-potentials and might be the best choice for cellular intervention to promote tendon-to-bone healing [40]. Chen et al. [14] have shown that TSCs could promote tendon-to-bone healing in rotator cuff repair, with a significant up-regulation of gene expression in osteoblasts, chondrocytes, and tenocytes, with an increase in new bone and fibrocartilage. In our study, the histological results showed that collagen fibers in BMP2-CHS with TSCs group were more orderly and denser, and there were more new bone and fibrocartilage. CHS acted as a carrier for BMP2 and TSCs to retain growth factors and stem cells at the target site for a long time, providing initial support for tissue regeneration. In addition, CHS reduced adverse effects such as extensive heterotopic ossification brought by BMP2 [4,41]. Because of the manipulation of hydrogel, the explosive release of growth factors caused by pressing the sponge or patch was avoided. Several previous studies have demonstrated the effectiveness of collagen hydrogel as a BMP2 carrier [42,43]. Finally, the biomechanical test results showed that BMP2-CHS with TSCs could significantly enhance the biomechanical strength between the tendon and bone.

There were some limitations in this study. First, our acute injury and repair model does not reflect chronic degenerative rotator cuff tears, and the animal healing process may not reflect the patient's condition. Secondly, the hydrogel could not effectively reduce the stress concentration between bone and tendon, which is one of the focuses of our future work. Third, we did not evaluate the effectiveness of BMP2 alone. However, previous studies have showed that the effect of adding BMP2 to the vector was better than that of the control group [42]. Based on this finding, we did not set up a separate BMP2 group.

Taken together, the BMP2-CHS with TSCs described in this study greatly improved the repair of rotator cuff injury, promoted tendon-to-bone healing, and enhanced the biomechanical strength of tendon-to-bone connection. Ultimately, these results may contribute to the application of tissue engineering techniques to enhance tendon-to-bone healing.

5. Conclusions

A new hydrogel scaffold, CHS, has been developed using tissue engineering techniques in this study. The material characterization experiments showed that the CHS had good biocompatibility, degradability, and special porous properties. The CHS promoted the proliferation of TSCs during in vitro expansion. Moreover, the CHS could significantly promote chondrogenic differentiation of TSCs after incorporation of BMP2 and enhance the tendon-to-bone healing of rotator cuff in vivo. Therefore, we suggest that the CHS may be applied for tissue engineering for effective repair or possible regeneration of rotator cuff tears.

Ethics approval

All experimental protocols involving animals were approved by the Ethics Committee of Wuhan Fourth Hospital (Approval number: KY2021-065-01) and performed in accordance with relevant guidelines and regulations.

Consent for publication

Not applicable.

Funding

This research was funded by Foundation of Department of Science and Technology of Hubei Province (2021CFB520) and the Start-up Research Grant (Wuhan Fourth Hospital Young Backbone Talent Training Program).

Data availability statement

All data generated or analyzed during this study are included in article.

CRedit authorship contribution statement

Qingsong Zhang: Writing – original draft, Supervision, Software, Project administration, Investigation, Funding acquisition, Formal analysis, Conceptualization. **Huawei Wen:** Writing – review & editing, Writing – original draft, Validation, Supervision, Resources, Project administration, Methodology, Investigation, Formal analysis, Conceptualization. **Guangyang Liao:** Visualization, Software, Resources, Methodology, Data curation. **Xianhua Cai:** Writing – review & editing, Visualization, Validation, Supervision, Software, Resources, Project administration, Methodology.

Declaration of competing interest

The authors declare that they have no known competing financial interests or personal relationships that could have appeared to influence the work reported in this paper.

References

- [1] M.D. Galetta, R.E. Keller, O.D. Sabbag, S.E. Linderman, M.S. Fury, G. Medina, E.A. O'Donnell, T.T.W. Cheng, E. Harris, L.S. Oh, Rehabilitation variability after rotator cuff repair, *J. Shoulder Elbow Surg.* 30 (6) (2021) e322–e333.
- [2] W. Chen, Y. Sun, X. Gu, J. Cai, X. Liu, X. Zhang, J. Chen, Y. Hao, S. Chen, Conditioned medium of human bone marrow-derived stem cells promotes tendon-bone healing of the rotator cuff in a rat model, *Biomaterials* 271 (2021) 120714.
- [3] Y.H. Kim, W.G. Jang, S.H. Oh, J.W. Kim, M.N. Lee, J.H. Song, J.W. Yang, Y. Zang, J.T. Koh, Fenofibrate induces PPARalpha and BMP2 expression to stimulate osteoblast differentiation, *Biochem. Biophys. Res. Commun.* 520 (2) (2019) 459–465.
- [4] M.H. O'Brien, E.H. Dutra, S. Mehta, P.J. Chen, S. Yadav, BMP2 is required for postnatal maintenance of osteochondral tissues of the temporomandibular joint, *Cartilage* 13 (2, suppl) (2021) 734S–743S.
- [5] H. Shen, J. Shi, Y. Zhi, X. Yang, Y. Yuan, J. Si, S.G.F. Shen, Improved BMP2-CPC-stimulated osteogenesis in vitro and in vivo via modulation of macrophage polarization, *Mater. Sci. Eng., C* 118 (2021) 111471.
- [6] S.T. Bianco, H.L. Moser, L.M. Galatz, A.H. Huang, Biologics and stem cell-based therapies for rotator cuff repair, *Ann. N. Y. Acad. Sci.* 1442 (1) (2019) 35–47.
- [7] L. Audige, S. Aghlmandi, C. Grobet, T. Stojanov, A.M. Muller, Q. Felsch, J. Gleich, M. Flury, M. Scheibel, Prediction of shoulder stiffness after arthroscopic rotator cuff repair, *Am. J. Sports Med.* 49 (11) (2021) 3030–3039.
- [8] M. Fan, L. Jia, M. Pang, X. Yang, Y. Yang, S. Kamel Elyzayati, Y. Liao, H. Wang, Y. Zhu, Q. Wang, Injectable adhesive hydrogel as photothermal-derived antigen reservoir for enhanced anti-tumor immunity, *Adv. Funct. Mater.* 31 (20) (2021).
- [9] A. Zheng, D. Wu, M. Fan, H. Wang, Y. Liao, Q. Wang, Y. Yang, Injectable zwitterionic thermosensitive hydrogels with low-protein adsorption and combined effect of photothermal-chemotherapy, *J. Mater. Chem. B* 8 (46) (2020) 10637–10649.
- [10] C. Wang, Y. Zhang, G. Zhang, W. Yu, Y. He, Adipose stem cell-derived exosomes ameliorate chronic rotator cuff tendinopathy by regulating macrophage polarization: from a mouse model to a study in human tissue, *Am. J. Sports Med.* 49 (9) (2021) 2321–2331.
- [11] E.T. Hurlley, D. Lim Fat, C.J. Moran, H. Mullett, The efficacy of platelet-rich plasma and platelet-rich fibrin in arthroscopic rotator cuff repair: a meta-analysis of randomized controlled trials, *Am. J. Sports Med.* 47 (3) (2019) 753–761.
- [12] D.M. Kim, I.K. Shim, M.J. Shin, J.H. Choi, Y.N. Lee, I.H. Jeon, H. Kim, D. Park, E. Kholinne, K.H. Koh, A combination treatment of raloxifene and vitamin D enhances bone-to-tendon healing of the rotator cuff in a rat model, *Am. J. Sports Med.* 48 (9) (2020) 2161–2169.
- [13] S.A. Qin, B. Sb, W. Wen, C. Ala, B. Jx, The role of tendon derived stem/progenitor cells and extracellular matrix components in the bone tendon junction repair, *Bone* (2021).
- [14] L. Chen, C. Jiang, S.R. Tiwari, A. Shrestha, P. Xu, W. Liang, Y. Sun, S. He, B. Cheng, TGIF1 gene silencing in tendon-derived stem cells improves the tendon-to-bone insertion site regeneration, *Cell. Physiol. Biochem.* 37 (6) (2015) 2101–2114.
- [15] A. Msd, A. Mbd, A. Aod, B. Asjd, C. Jmm, Arthroscopic debridement for management of massive, irreparable rotator cuff tears: a systematic review of outcomes - ScienceDirect, *JSES Rev. Reports Techniques* (2022).
- [16] A. Romeo, J. Easley, R. Dan, E. Hackett, K. Mcgilvray, Rotator cuff repair using a bioresorbable nanofiber interposition scaffold: a biomechanical and histological analysis in sheep, *J. Shoulder Elbow Surg.* (2021).
- [17] N. Weir, B. Stevens, S. Wagner, A. Miles, G. Ball, C. Howard, J. Chemmarappally, M. Mcginny, C. Tinsley, A.J. Hargreaves, Aligned poly-L-lactic acid nanofibers induce self-assembly of primary cortical neurons into 3D cell clusters, *ACS Biomater. Sci. Eng.* 8 (2) (2022) 765–776.
- [18] C.H. Park, Three-dimensional digital light-processing bioprinting using silk fibroin-based bio-ink: recent advancements in biomedical applications, *Biomedicine* 10 (2022).
- [19] C.Y. Wang, Y.C. Chiu, K.X. Lee, Y.A. Lin, M.Y. Shie, Biofabrication of gingival fibroblast cell-laden collagen/strontium-doped calcium silicate 3D-printed Bi-layered scaffold for osteoporotic periodontal regeneration, *Biomedicine* 9 (4) (2021) 431.
- [20] A. Bharadwaz, A.C. Jayasuriya, Recent Trends in the Application of Widely Used Natural and Synthetic Polymer Nanocomposites in Bone Tissue Regeneration. *Materials Science & Engineering, C. Materials for Biological Applications*, 2020, 110–.
- [21] B. Ye, B. Wu, Y. Su, T. Sun, X. Guo, Recent advances in the application of natural and synthetic polymer-based scaffolds in musculoskeletal regeneration, *Polymers* 14 (21) (2022) 4566.
- [22] E.M. Trifanova, M.A. Khvorostina, A.O. Mariyanats, A.V. Sochilina, M.E. Nikolaeva, E.V. Khaydukov, R.A. Akasov, V.K. Popov, Natural and synthetic polymer scaffolds comprising upconversion nanoparticles as a bioimaging platform for tissue engineering, *Molecules* 27 (19) (2022) 6547.
- [23] K. Zhang, Q. Peng, Z. Fang, L. Gu, L. Bian, Structurally dynamic hydrogels for biomedical applications: pursuing a fine balance between macroscopic stability and microscopic dynamics, *Chem. Rev.* 121 (18) (2021) 11149–11193.
- [24] Shuai, C. A.; We, B.; Ye, C.; Xm, D.; Cf, A., Chondroitin sulfate modified 3D porous electrospun nanofiber scaffolds promote cartilage regeneration - ScienceDirect. *Mater. Sci. Eng., C* 118..
- [25] V. Vassallo, A. Tsianaka, N. Alessio, Jana Grübel, M. Cammarota, M. Tovar, G. E, A. Southan, C. Schiraldi, Evaluation of novel biomaterials for cartilage regeneration based on gelatin methacryloyl interpenetrated with extractive chondroitin sulfate or unsulfated biotechnological chondroitin, *J. Biomed. Mater. Res., Part A* 110 (6) (2022) 1210–1223.
- [26] M.O.G. Ferreira, A.B. Ribeiro, M.S. Rizzo, A.C.D.J. Oliveira, J.A. Osajima, L.M. Estevinho, E.C. Silva-Filho, Potential wound healing effect of gel based on chicha gum, chitosan, and mauritia flexuosa oil, *Biomedicine* 10 (4) (2022) 899.
- [27] J.-H. Yea, T.S. Bae, B.J. Kim, Y.W. Cho, C.H. Jo, Regeneration of the rotator cuff tendon-to-bone interface using umbilical cord-derived mesenchymal stem cells and gradient extracellular matrix scaffolds from adipose tissue in a rat model, *Acta Biomater.* 114 (2020) 104–116.
- [28] E. Pugliese, I. Sallent, S. Ribeiro, A. Trotier, S.H. Korntner, Y. Bayon, D.I. Zeugolis, Development of three-layer collagen scaffolds to spatially direct tissue-specific cell differentiation for enthesis repair, *Mater Today Bio* 19 (2023) 100584.
- [29] Y. Hirakawa, T. Manaka, K. Orita, Y. Ito, K. Ichikawa, H. Nakamura, The accelerated effect of recombinant human bone morphogenetic protein 2 delivered by β -tricalcium phosphate on tendon-to-bone repair process in rabbit models, *J. Shoulder Elbow Surg.* (2018). S1058274617307723.
- [30] C. Jiang, F. Hu, X. Xia, X. Guo, Prognostic value of alkaline phosphatase and bone-specific alkaline phosphatase in breast cancer: a systematic review and meta-analysis, *Int. J. Biol. Markers* 38 (1) (2023) 25–36.
- [31] B. Huang, H. Liu, S. Chan, J. Liu, J. Gu, M. Chen, L. Kuang, X. Li, X. Zhang, J. Li, RUNX2 promotes the suppression of osteoblast function and enhancement of osteoclast activity by multiple myeloma cells, *Med. Oncol.* 40 (4) (2023).
- [32] H. Sugimoto, S. Fukuda, S. Yokawa, M. Hori, H. Ninomiya, T. Sato, K. Miyazawa, T. Kawai, T. Furuno, S. Inouye, Visualization of osteocalcin and bone morphogenetic protein 2 (BMP2) secretion from osteoblastic cells by bioluminescence imaging, *Biochem. Biophys. Res. Commun.* 635 (2022) 203–209.
- [33] C. Arvinius, A. Civantos, C. Rodríguez-Bobada, F.J. Rojo, D. Pérez-Gallego, Y. Lopez, F. Marco, Enhancement of in vivo supraspinatus tendon-to-bone healing with an alginate-chitin scaffold and rhBMP-2, *Injury* 52 (1) (2021) 78–84.
- [34] R. Yang, G. Li, C. Zhuang, P. Yu, T. Ye, Y. Zhang, P. Shang, J. Huang, M. Cai, L. Wang, W. Cui, L. Deng, Gradient bimetallic ion-based hydrogels for tissue microstructure reconstruction of tendon-to-bone insertion, *Sci. Adv.* 7 (26) (2021).
- [35] G. Pratama, V. Vaghjiani, Y.T. Jing, H.L. Yu, J. Chan, C. Tan, P. Murthi, C. Gargett, U. Manuelpillai, Changes in culture expanded human amniotic epithelial cells: implications for potential therapeutic applications, *PLoS One* 6 (2011).

- [36] X. Yao, S. K. S. Yu, J. Luo, J. Guo, J. Lin, G. Wang, Z. Guo, Y. Ye, F. Guo, Chondrocyte ferroptosis contribute to the progression of osteoarthritis, *J. Orthopaedic Translat.* 27 (2021) 33–43.
- [37] K. Suzuki, H. Kaseyama-Takemoto, Simultaneous production of N-acetylheparosan and recombinant chondroitin using gene-engineered *Escherichia coli* K5, *Heliyon* 9 (4) (2023) e14815.
- [38] C.M.L.D. Padilla, M.J. Coenen, A. Tovar, R.E.D.L. Vega, C.H. Evans, S.A. Müller, Picrosirius red staining: revisiting its application to the qualitative and quantitative assessment of collagen type I and type III in tendon, *J. Histochem. Cytochem.* 69 (10) (2021) 633–643.
- [39] P.K. Nguyen, F. Deng, S. Assi, P. Paco, S. Fink, C. Stockwell, C.K. Kuo, Phenotype stability, expansion potential, and senescence of embryonic tendon cells in vitro, *J. Orthop. Res.* 40 (7) (2022) 8.
- [40] Y.F. Rui, P.P. Lui, Y.W. Lee, K.M. Chan, Higher BMP receptor expression and BMP-2-induced osteogenic differentiation in tendon-derived stem cells compared with bone-marrow-derived mesenchymal stem cells, *Int. Orthop.* 36 (5) (2012) 1099–1107.
- [41] Subbiah, R.; Ruehle, M.; Klosterhoff, B. S.; Lin, A. S.; Hettiaratchi, M. H.; Willett, N. J.; Bertassoni, L. E.; García, A.; Guldberg, R. E., Triple Growth Factor Delivery Promotes Functional Bone Regeneration Following Composite Musculoskeletal Trauma. Social Science Electronic Publishing..
- [42] J.G. Kim, H.J. Kim, S.E. Kim, J.H. Bae, Y.J. Ko, J.H. Park, Enhancement of tendon-bone healing with the use of bone morphogenetic protein-2 inserted into the suture anchor hole in a rabbit patellar tendon model, *Cytotherapy* 16 (6) (2014) 857–867.
- [43] Y. Park, S. Lin, Y. Bai, S. Moeinzadeh, S. Kim, J. Huang, U. Lee, N.F. Huang, Y.P. Yang, Dual delivery of BMP2 and IGF1 through injectable hydrogel promotes cranial bone defect healing, *Tissue Eng.* 28 (17–18) (2022) 760–769.